First-principles study of hydrogen vacancies in sodium alanate with Ti substitution

2010 J. Phys.: Condens. Matter 22 205503

(http://iopscience.iop.org/0953-8984/22/20/205503)

J. Phys.: Condens. Matter **22** (2010) 205503 (8pp) doi:10.1088/0953-8984/22/20/205503

First-principles study of hydrogen vacancies in sodium alanate with Ti substitution

Hao Wang, Akinori Tezuka, Hiroshi Ogawa and Tamio Ikeshoji

Research Institute for Computational Sciences (RICS), National Institute of Advanced Industrial Science and Technology (AIST), AIST Tsukuba Central 2, Umezono 1-1-1, Tsukuba, Ibaraki 305-8568, Japan

E-mail: kou.ou@imr.tohoku.ac.jp (Hao Wang)

Received 11 February 2010, in final form 13 March 2010
Published 30 April 2010
Online at stacks.iop.org/JPhysCM/22/205503

Abstract

In order to clarify the effect of hydrogen vacancies on the stability and structure of sodium alanate, $NaAlH_4$, with and without Ti substitution for Al, first-principles electronic structure calculations were carried out. The relative thermodynamic stability of the Ti dopant and the H vacancy in a supercell was obtained. For the Ti-doped $Na_{16}Al_{16}H_{64}$ supercell calculations, it was preferable to perform the initial substitution with a cluster of $TiAlH_n$. We showed that substitution of a Ti atom for an Al atom in $Na_{16}Al_{15}TiH_{63}$ with H vacancies increases the stability of the structure. A density of states analysis revealed weakening of the bond strength corresponding to increase in the bond length.

(Some figures in this article are in colour only in the electronic version)

1. Introduction

Hydrogen is a very attractive energy source and energy mediator because it has the highest ratio of valence electrons to protons among all elements as well as very high energy gain per electron [1]. Conventional methods of hydrogen storage involve the use of high-pressure hydrogen gas tanks or cryogenic tanks for storing liquid hydrogen [2, 3]. Intermetallic hydrides are among the on-board hydrogen storage candidates; specifically, light elements such as lithium, boron, sodium and aluminum can form stable compounds with hydrogen. Owing to the high mass density of hydrogen in these light-element hydrides, extensive experimental and theoretical research is being carried out on using these hydrogen storage materials for automobiles. However, hydrogen in these materials is held by strong covalent or ionic bonds. Consequently, the hydrogen desorption temperatures are high and the kinetic processes are slow. Recently, sodium alanate, $NaAlH_4$, has attracted considerable attention as a hydrogen storage material. It has moderate hydrogen gravimetric capacity (5.6 wt%) and relatively rapid hydrogenation kinetics. Although temperatures higher than room temperature are required for the desorption of hydrogen, it has served as a prototype for providing an understanding of the underlying mechanism of dehydrogenation and rehydrogenation in materials with similar structures and compositions.

In order to make the absorption/desorption process reversible under practical conditions, $NaAlH_4$ must be doped with a catalyst. Bogdanovic and Schwickardi have shown experimentally that the decomposition temperature of $NaAlH_4$ is reduced and the release of hydrogen becomes reversible when $NaAlH_4$ is doped with TiO_2 [4]. Furthermore, the addition of a small amount of $TiCl_3$ to sodium alanate has also been found not only to make the reaction reversible, but also to lower the hydrogen desorption temperature markedly [4]. Doping with Ti has yielded experimental dehydriding rates of 1 wt% h^{-1} at 383 and 433 K for the first and second decomposition steps, respectively, but at the cost of lower hydrogen capacity (~4.5 wt%) [2]. Majzoub and Gross have reported that Ti is atomically dispersed in $NaAlH_4$, both as a substitute ion and perhaps as $TiAl_3$, by the highly exothermic formation of sodium halides [5]. Such an atomically dispersed structure is consistent with x-ray diffraction studies suggesting that Ti may be substituted into bulk $NaAlH_4$ [6]. However, conflicting results have been reported on the location of Ti in sodium alanate. In some experiments, Ti has been found to remain on the surface [4, 7], whereas Ti has been found in other studies to occupy the bulk Na site [6, 8–10].

To date, several research groups have investigated $NaAlH_4$ theoretically. It is conventionally considered that an ionic bond forms between the Na^+ cation and the AlH_4^- anion. Aguayo *et al* have studied the electronic band structure of pure sodium alanate and suggested that the ionic nature of sodium alanate is the result of long-range Coulomb interactions between Na^+, Al^{3+} and H^- ions. They found that the Al–H bond is sensitive to substitutions and defects [11]. On the basis of electronic structure calculations, Íñiguez *et al* proposed a model in which Ti is substituted for the Na atom in sodium alanate [9, 12]. On the other hand, Løvvik *et al* concluded from electronic structure calculations that Ti-doped structures are thermodynamically unstable in comparison with pure sodium alanate, and that among the various possible doped structures, that based on the substitution of Ti for Al is the most suitable metastable model [10, 13]. According to Araujo *et al*, this discrepancy between the two studies arose from the choice of reference states [14], that is, Ti occupies the Na site preferentially over the Al site when the atomic energies are used as the reference. However, using the cohesive energies of Al, Na and Ti leads to the Al site being favored.

It has been shown theoretically that substitution for metal atoms near the surface is favored over substitution for metal atoms in the bulk [13]. However, Sun *et al* demonstrated experimentally that the introduction of variable valence transition metal cations into $NaAlH_4$ leads to the formation of Na^+ vacancies in the bulk hydride lattice [6]. On the basis of an experimental study, Palumbo *et al* suggested that a model that aims to explain the decomposition reactions and kinetics of doped $NaAlH_4$ should take into account hydrogen mobility, trapping and the stoichiometric defects [15]. Íñiguez *et al* have shown theoretically that in Ti-doped $NaAlH_4$, Ti atoms bind with more hydrogen atoms than Al atoms can in pure $NaAlH_4$ and introduce a number of vacancies; furthermore, they have reported that decomposition of sodium alanate occurs at a lower temperature [16]. From these studies, we expect hydrogen vacancies (H vacancies) to play an important role in the desorption of hydrogen from sodium alanate.

In the theoretical research carried out to date on Ti-doped sodium alanate, only the location of Ti and its effects on the desorption of hydrogen have been considered. The effects of H vacancies due to the doping of Ti into bulk $NaAlH_4$ have not been clearly elucidated, although the effects of metal vacancies have been researched. In this study, we investigate H point defects in Ti-doped sodium alanate by means of first-principles calculations. The main objective of this study is to clarify the geometrical and electronic structures of sodium alanate with inclusion of one H vacancy, with and without Ti substitution for Al in a supercell.

2. Methodology

We performed electronic structure calculations based on density functional theory (DFT). The projector augmented wave (PAW) method embodied in the Quantum MAterials Simulator (QMAS) code was employed [17]. The generalized gradient approximation (GGA) with the PBE96 exchange–correlation functional was adopted [18, 19]. A $2 \times 2 \times 1$ supercell for the lattice unit of $Na_4Al_4H_{16}$ ($Na_{16}Al_{16}H_{64}$ as the whole) was built to avoid drastic structural changes arising from the introduction of a dopant and/or a H vacancy. For a supercell containing both a Ti dopant and H vacancy, an appropriate distance between them was adopted. The coordinates of the atoms and the lattice constants of the supercell were optimized using the Hellmann–Feynman forces acting on the atoms and the stresses on the supercell. This optimization was performed without any symmetry constraints. The plane wave cutoff energy was set to 35 Ryd to obtain sufficiently high accuracy, and a k-point grid of $2 \times 2 \times 2$ (less than 0.4 $Å^{-1}$) was applied. The self-consistent-charge distance, force and stress thresholds in the SCF calculations were set to 1.5×10^{-8} electrons $Å^{-3}$, 0.005 eV $Å^{-1}$ and 0.001 eV $Å^{-3}$, respectively, to obtain good convergence. Since we adopted a neutral vacancy here, no background charge was required. The ground state phases, $Im\bar{3}m$ Na metal, $Fm\bar{3}m$ Al metal and $P6_3/mmc$ Ti metal, were used to determine enthalpies. For a diatomic H_2 molecule, a 10 Å × 10 Å × 10 Å cubic unit cell having energetic convergence with respect to the cell size was adopted.

3. Results and discussion

3.1. Crystal structure and stability

$NaAlH_4$ has space group $I4_1/a$ with four formula units per primitive cell. The Wyckoff sites for Na, Al and H are $4a$, $4b$ and $16f$, respectively. The atomic configuration of $NaAlH_4$ in the supercell is shown in figure 1(a). Since substitution of Ti atom for an Al atom, where the two atoms have similar ionic radii and formal valences, is favored over substitution of Ti for a larger, monovalent Na atom, we adopted substitution of Al in this calculation, as Løvvik *et al* did [10]. The hydrogen atom, labeled 'H', is replaced with a vacancy, and the Al atom, labeled 'Al1', is replaced with a Ti atom. This single-atom replacement is referred to as 'atom substitution' in this text. If the Al atoms labeled 'Al1' and 'Al2' and the hydrogen atoms bound to them are replaced with an $AlTiH_n$ ($n = 7, 8$) cluster, this is referred to as 'cluster substitution', which is explained in detail in section 3.1.1.

3.1.1. Cluster substitution. It is well known that determining the global minimum of the potential energy surface of a complex system is a central problem in computational physics, chemistry and biology. Determination of the global minimum in calculations is expensive, primarily because the number of local minima increases exponentially with the number of atoms in the system. For a large supercell containing structural disorder, for example, point defects, the system can easily become trapped in one of these local minima. Therefore, simple atom substitution in the calculation possibly does not provide the global minimum energy of the system. Thus, we decided to substitute a cluster whose structure had been optimized prior to the substitution for a part including Al and several other atoms in the supercell. Such a replacement is expected to yield more stable Ti-doped sodium alanate with H vacancies.

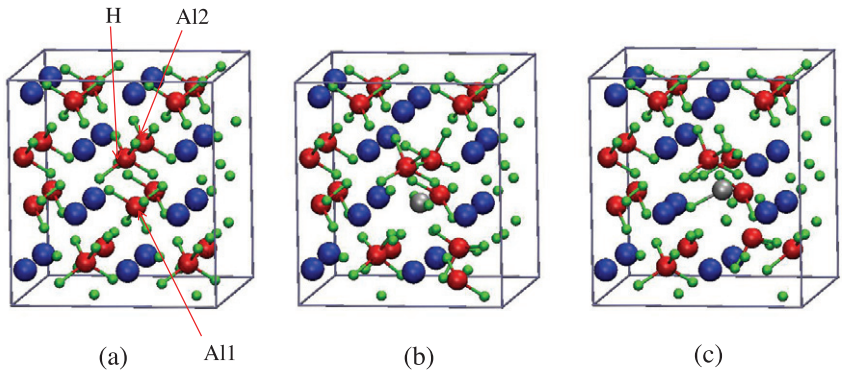

Figure 1. (Color online) Crystal structures in the supercell. (a) $Na_{16}Al_{16}H_{64}$. (b) Atom-substituted $Na_{16}Al_{15}TiH_{64}$. (c) Cluster-substituted $Na_{16}Al_{15}TiH_{64}$. Red (middle), blue (big) and green (small) balls denote Al, Na and H atoms, respectively. The indicated hydrogen is replaced with a vacancy and the Al atom marked 'Al1' is replaced with a Ti atom. In the case of cluster substitution, the Al atoms labeled 'Al1' and 'Al2' and the hydrogen atoms bound to them are replaced with an $TiAlH_n$ ($n = 7, 8$) cluster.

Table 1. Optimized lattice parameters and enthalpies of formation and substitution for $Na_{16}Al_{16-m}Ti_mH_{64-n}$ ($m = 0$, 1 and $n = 0$, 1). H^v represents a supercell with one H vacancy, the location of which is shown in figure 1. Ti substitution for Al without a H vacancy and with a H vacancy is expressed as Ti@Al and Ti@Al + H^v, respectively; this Al site is also shown in figure 1. Atom substitution and cluster substitution are denoted by 'atm' and 'cls', respectively.

	Lattice vectors (Å)			Lattice angles (deg)					
	a	b	c	α	β	γ	V (Å^3)	H_{Form} (eV)	H_{Subst} (eV)
$Na_{16}Al_{16}H_{64}$ (pure)	10.0	10.0	11.1	90	90	90	1110	−12.30	
Others' exp.[a]	9.96	9.96	11.15						
Others' calc.[b]	9.90	9.90	10.89						
Others' calc.[c]	10.0	10.0	11.11	90				−17.51	
Others' calc.[d]	10.0	10.0	11.12	90				−13.09	
Others' calc.[e]							1115.2	−13.18	
$Na_{16}Al_{16}H_{63}$ (H^v)	9.93	9.94	10.96	89.99	89.96	89.96	1081.8	−10.60	1.71
$Na_{16}Al_{15}TiH_{64}$									
Ti@Al(atm)	9.91	9.94	10.88	89.46	89.90	89.60	1071.2	−11.29	1.02
Ti@Al(cls)	9.83	10.20	11.10	89.75	89.99	88.56	1112.0	−11.57	0.74
Others' calc.[c]	10.02	10.02	10.93					−16.02	1.49
$Na_{16}Al_{15}TiH_{63}$									
Ti@Al + H^v (atm)	9.93	9.93	10.91	89.97	89.98	90	1075.1	−11.43	0.88
Ti@Al + H^v (cls)	10.11	10.04	11.09	89.91	89.57	89.72	1126.2	−11.68	0.63
Others' calc.[c]	9.94	9.94	11.07	89.8				−15.75	1.77

[a] Reference [21]. [b] Reference [20]. [c] Reference [10]. [d] Reference [24]. [e] Reference [25].

We calculated the electronic structures of $TiAlH_n$ ($n = 7, 8$) clusters to find their most stable structures. Structural optimization was carried out by using a cubic supercell of 20 Å, for which it had been verified that the effects of the periodic boundary conditions could be ignored. Even though the formal charge of the corresponding part of the supercell was 2− ($2AlH_4^-$), we calculated the electronic structures of various charged clusters, namely, $TiAlH_8^{2-}$, $TiAlH_8^-$, $TiAlH_8$, $TiAlH_8^+$ and $TiAlH_8^{2+}$. The stability increased in the order of 2+ to 2− after structural optimization. The stability of $TiAlH_7$ exhibited the same order. To ensure smooth substitution of the cluster, that is, to prevent strong interactions between the cluster and the atoms around it, the Al–Ti line in the cluster was set along the line connecting the initial two Al atom positions in the corresponding AlH_4^-–AlH_4^- complex, followed by rotation of the cluster around the Al–Ti line through an appropriate angle. To maintain supercell neutrality, the total charge of the supercell was set to zero after substitution of the relaxed charged clusters. Full relaxation of all cases showed that the structures of $TiAlH_8^-$ and $TiAlH_7^-$ were the most stable after substitution. The relaxed atom-substituted and cluster-substituted $Na_{16}Al_{15}TiH_{64}$ supercells are presented in figures 1(b) and (c), respectively. The geometries of the atoms around Ti in various relaxed structures (in vacuum and in the supercell) are shown in figure 2. The initial cluster structures were altered after relaxation in both $Na_{16}Al_{15}TiH_{64}$ and $Na_{16}Al_{15}TiH_{63}$. Lower energy was obtained for cluster substitution compared with atom substitution.

3.1.2. Lattice changes induced by substitution. Table 1 lists the lattice constants of the supercells of the various $NaAlH_4$ systems and their enthalpies of formation and substitution. In the table, H^v denotes substitution of a single H vacancy, whose location is shown in figure 1. Ti@Al represents the substitution of a Ti atom for an Al atom. When a

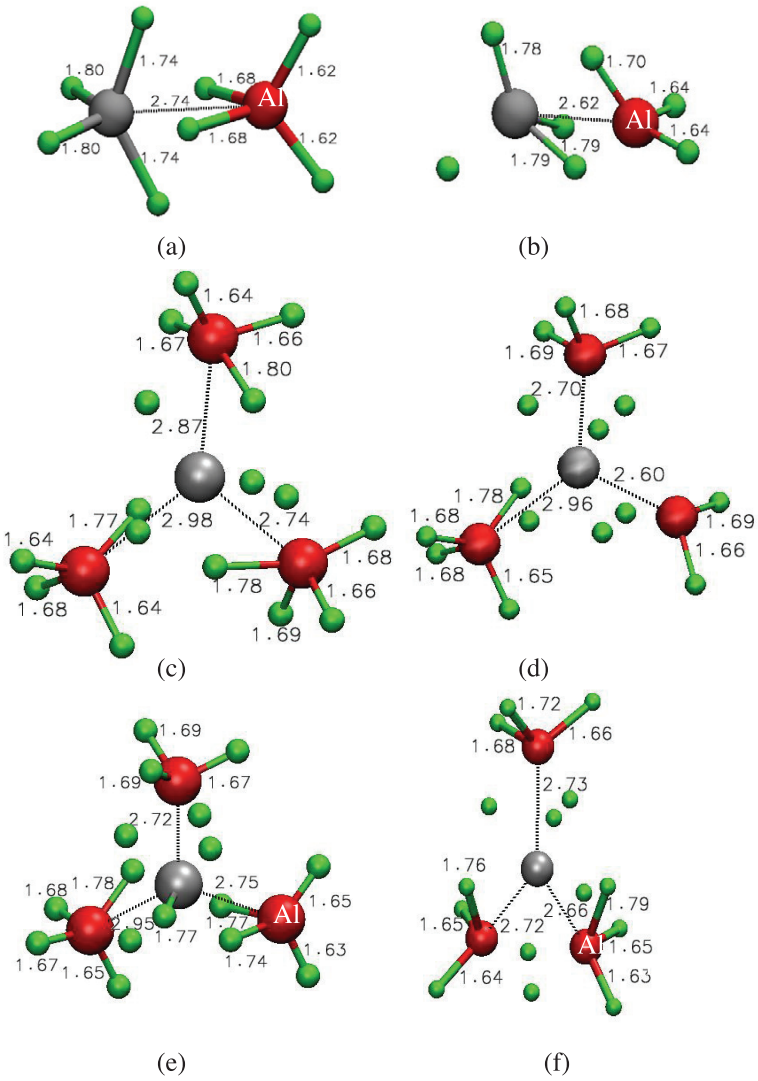

Figure 2. (Color online) Geometries of ((a), (b)) relaxed clusters in vacuum and ((c)–(f)) atoms around Ti in several systems. (a) $TiAlH_8^-$, (b) $TiAlH_7^-$, (c) part of the relaxed $Na_{16}Al_{15}TiH_{64}$ with Ti atom substitution, (d) part of the relaxed $Na_{16}Al_{15}TiH_{63}$ with Ti atom substitution, (e) part of the relaxed $Na_{16}Al_{15}TiH_{64}$ with cluster substitution and (f) part of the relaxed $Na_{16}Al_{15}TiH_{63}$ with cluster substitution. Red (big), gray and green (small) balls denote Al, Ti and H atoms, respectively. Al atoms labeled as 'Al' in (a) and (e), as well as in (b) and (f), are the same atom. The value beside a bond or line is the distance between the two atoms.

H vacancy is introduced to Ti@Al, it is represented as $Ti@Al + H^v$; this Al atom, which is replaced by substitution, is shown in figure 1. The terms 'cls' and 'atm' represent cluster substitution and atom substitution, respectively. The lattice parameters of the supercell $Na_{16}Al_{16}H_{64}$ obtained from our calculations were $a = b = 10.0$ Å and $c = 11.1$ Å, which are in good agreement with the values derived from experimental data, namely, 9.96, 9.96 and 11.15, respectively, as well as with the calculation results obtained in previous studies [11, 20–23]. Cluster-substituted $Ti@Al(Na_{16}Al_{15}TiH_{64})$ and $Ti@Al + H^v(Na_{16}Al_{15}TiH_{63})$ had larger lattice constants than the corresponding supercells with simple Ti atom substitution; the only exception was the a lattice vector in the case of atomic substitution of Ti for Al. Since Ti atoms are slightly larger than Al atoms, the volume change arising from cluster substitution of Ti@Al(cls) expanded the lattice to a size larger than the lattice of $Na_{16}Al_{16}H_{64}$. This result indicates that more accurate lattice constants can be obtained by cluster substitution than atom substitution. In comparison with the volume of Ti@Al(atm), the volume of Ti@Al(cls) for the addition of 6.25 mol% Ti was closer to the experimental value of 1151 $Å^3$ for the addition of 6.4 mol% to bulk [6].

3.1.3. Stability and enthalpies of formation and substitution. The formation enthalpy is defined as the difference between the total energy of a system and the energy of the individual atoms in their standard states. It is given by

$$H_{\mathrm{Form}}(Na_{16}Al_{16-l}Ti_mH_{64-n}) = E(Na_{16}Al_{16-l}Ti_mH_{64-n}) - \left(16E(\mathrm{Na}) + (16-l)E(\mathrm{Al}) + mE(\mathrm{Ti}) + \frac{(64-n)}{2}E(H_2)\right). \quad (1)$$

The substitution enthalpy is the difference between the formation enthalpy of the doped compounds and that of the original compounds. It is given by

$$H_{\text{Subst}}(\text{Na}_{16}\text{Al}_{16-l}\text{Ti}_m\text{H}_{64-n}) = E(\text{Na}_{16}\text{Al}_{16-l}\text{Ti}_m\text{H}_{64-n}) + lE(\text{Al}) + \frac{n}{2}E(\text{H}_2) - (E(\text{Na}_{16}\text{Al}_{16}\text{H}_{64}) + mE(\text{Ti})). \quad (2)$$

Thus, the higher the formation enthalpy of a doped compound, the less stable it is. Similarly, the lower the substitution enthalpy, the easier it is to dope the compound.

Let us consider the formation enthalpies listed in table 1. From these values, it is evident that all doped compounds are less stable than $NaAlH_4$ itself. H^v shows the most unfavorable formation enthalpy. Its stability increases significantly after doping with Ti, considering the formation enthalpy. The formation enthalpy of Ti@Al decreases after introduction of a H vacancy. Thus, Ti-doped $NaAlH_4$ with a H vacancy has greater stability.

Atom substitution and cluster substitution exhibited the same trend for the energy difference between Ti@Al and $\text{Ti@Al} + \text{H}^v$, although lower energy was obtained by cluster substitution. It is preferable to substitute initially with a pre-optimized cluster of $TiAlH_n$. A single substituted atom may be easily trapped in a local minimum structure. Henceforth, only the cluster substitution is discussed, unless mentioned otherwise.

After the relaxation of the substituted supercell, the $TiAl_3H_n$ complex was clearly observed (figures 1(b) and (c)), suggesting that the dehydrogenation of sodium alanate possibly starts from a $TiAl_3H_n$ complex structure, followed by decomposition into $TiAl_3$. This notion is supported by the results from a combined TEM–EDX and XAFS study that showed experimentally that Ti is atomically dispersed in the Al phase, forming a Ti–Al alloy [26, 27]. Complete dehydrogenation results in the formation of $TiAl_3$ dispersed in a predominantly Al phase [30]. Moreover, this $TiAl_3H_n$ precursor is consistent with the results for the theoretical surface study calculation by Liu *et al* that showed that rehydrogenation possibly starts from the dispersed $TiAl_3$ with subsequent formation of the $TiAl_3H_n$ complex [28, 29].

The substitution enthalpies calculated in this study differed from those calculated in some previous studies; these discrepancies might arise from the different initial configurations used. In this study, the Al atom, for which Ti is substituted, is not in the same AlH_4^- unit as the introduced H vacancy. In the calculation by Løvvik *et al*, a Ti atom was substituted for AlH in the AlH_4^- unit [10]. We calculated the enthalpies of formation and substitution by attempting to avoid interactions between the defect and the dopant, maintaining a sufficient distance between them.

The hydrogen-removal energy, that is, the difference between the formation enthalpies of the original system and the dehydrogenated system, of $Na_{16}Al_{16}H_{63}$ is 1.70 eV, which is consistent with the value of 1.7 eV in the Blomqvist *et al* result [31]; this high value is a consequence of the strong covalent bonds between Al and H atoms. In contrast, the hydrogen-removal energy of cluster-substituted Ti@Al is only −0.11 eV, due to the change in the geometrical and electronic structures caused by Ti substitution, as shown in figure 2, as well as by the density of states (DOS) discussed later. This is different from the Blomqvist *et al* result [31], which is a little above zero. The hydrogen-removal energy of Ti@Al is significantly lower because Ti weakens the strength of the covalent bond between Al and H atoms. In spite of the distinct selection of the energy reference, that is, the individual atomic energy, the same trend for the hydrogen-removal energy was observed in the Araújo *et al* study [20]. In the study by Íñiguez *et al*, a low formation enthalpy was obtained for a surface with H vacancies when a Ti catalyst was present [16]; this trend is similar to that in the results of our bulk calculation.

3.1.4. Bonding and stability. The bond length of Al–H in pure $Na_{16}Al_{16}H_{64}$ is 1.641 Å, which is shorter than the Al–H bond length in the clusters shown in figure 2. In the H^v supercell, the AlH_3 unit remains nearly tetrahedral with a bond length of 1.642–1.650 Å. Cluster-substituted Ti@Al contains one AlH_3 unit whereas $\text{Ti@Al} + \text{H}^v$ contains three AlH_3 units. An isolated AlH_3 cluster is characterized by enhanced stability (the energy gained by forming AlH_3 from AlH_2 is 3.56 eV, while that gained by forming AlH_4 from AlH_3 is only 1.13 eV [32]). The stability of the AlH_3 unit clearly causes the low enthalpies of formation and substitution, although both the bond length and angle in the supercell are different from those in the isolated AlH_3 cluster [32]. The higher stability of Ti@Al+H^v in comparison with Ti@Al can also be attributed to the stability of AlH_3. This is similar to the case of the Na vacancy in Moysés' study, in which it was found that the stability of the planar AlH_3 cluster is primarily responsible for the reduced hydrogen-removal energy for dehydrogenation of the $Na_{15}Al_{15}TiH_{64}$ supercell [20]. In the present study, it was found that there is no large variation in the distance between the labeled Al and Ti atoms in each part of figure 2. Considering the distance of 3.71 Å between AlH_4^- units in $Na_{16}Al_{16}H_{64}$, the distances between the Ti and Al atoms apparently decreased, as shown in figures 2(e) and (f). Furthermore, since the AlH_3 units formed have a distance from the Ti atom in the range of 2.62–2.73 Å, the formation of a bond between Ti and Al atoms can be inferred because the bond length between Ti and Al in the compound $TiAl_3$ is 2.722 Å [33].

The AlH_3 unit in the $TiAlH_7$ cluster was retained in cluster substitution and two more subsequently appeared, whereas the AlH_3 unit was broken down to AlH_2 in the case of Ti atom substitution. This is consistent with the result that the energy obtained from substituting a cluster into $\text{Ti@Al} + \text{H}^v$ is lower than that from Ti atom substitution.

With the increase in the average Ti–H bond length by 0.01 Å in $\text{Ti@Al} + \text{H}^v$ compared with the bond length in Ti@Al, the H atoms become less tightly bound, which can lead to more facile H_2 gas desorption; this result is in agreement with experimental studies [15, 16]. The introduction of a Ti atom and a vacancy in $Na_{16}Al_{15}TiH_{63}$ increased the stability of the structure and increased the number of deformed AlH_3 units, thus allowing more energetically favorable H_2 gas desorption. Thus, doping $Na_{16}Al_{16}H_{64}$ with a Ti atom and a vacancy is more effective than doping with either of them separately.

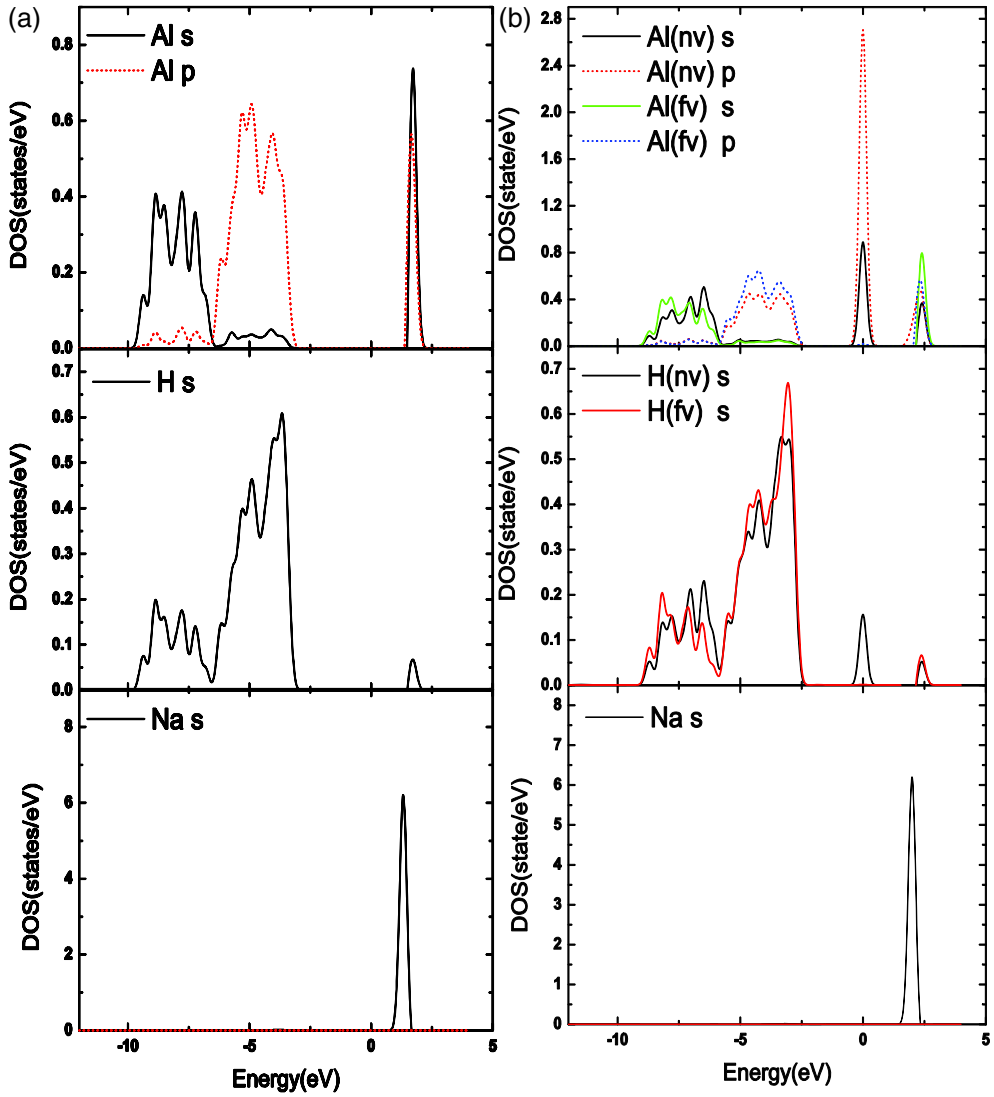

Figure 3. (Color online) Partial DOS of Na, Al and H atoms in (a) $Na_{16}Al_{16}H_{64}$ and (b) $Na_{16}Al_{16}H_{63}$. Solid and dotted lines denote s and p states, respectively. The term 'nv' denotes 'near the H vacancy', which signifies a distance of about 1.64 Å for the Al atom and 2.74 Å for the H atom from the vacancy position in $Na_{16}Al_{16}H_{64}$, whereas 'fv' indicates 'far from the H vacancy', which signifies a distance of about 3.95 Å for the Al atom and 7.50 Å for the H atom from the vacancy position in $Na_{16}Al_{16}H_{64}$. The Fermi energy was set to zero.

So far, we have considered only the electronic energy, not temperature effects. However, the reduced strength of the Ti–H bond observed here is expected to be related to the temperature required for hydrogen desorption. Although an optimized structure was found, other local minimum structures possibly exist with the same energy. Such a structure was inferred from the result of atom substitution. Although molecular dynamics (MD) calculations at a certain temperature could assist in more clearly understanding hydrogen desorption in the presence of a Ti catalyst, such first-principles MD calculations have a high cost because time resolution in the MD trajectory with more than 10 000 steps is necessary.

3.2. The density of states

Figure 3 shows the s and p partial DOS for Na, Al and H atoms in the supercells without and with a H vacancy. The solid and dotted lines denote the s and p states, respectively. In figure 3(a), the valence band of $Na_{16}Al_{15}TiH_{64}$ is split into two components. The H 1s and Al 3s states contribute to the lower-energy component, while hybridization between the Al 3p and H 1s states contributes to the higher-energy component. The appearance of Al and H peaks at the same energy indicates strong bonding between the Al and H atoms. The conduction band is dominated primarily by the Na 3s state. This may imply ionic bonding between the Na^+ and AlH_4^- units. The DOS of $Na_{16}Al_{16}H_{63}$, which is shown in figure 3(b), is similar to the DOS of $Na_{16}Al_{16}H_{64}$, except that there is a peak around the Fermi energy. This peak is attributed to the hybridization among the H 1s, Al 2p and Al 2s orbitals of atoms in the AlH_3 cluster, which includes the H vacancy. The introduction of a H vacancy also gives rise to an interaction between the Al and H orbitals in the conduction band. These can be attributed to the extra Al electron that remains after removal of the H atom. Since the DOS of the Na atom does not change after H vacancy doping, except for a shift to higher energy, it can be concluded

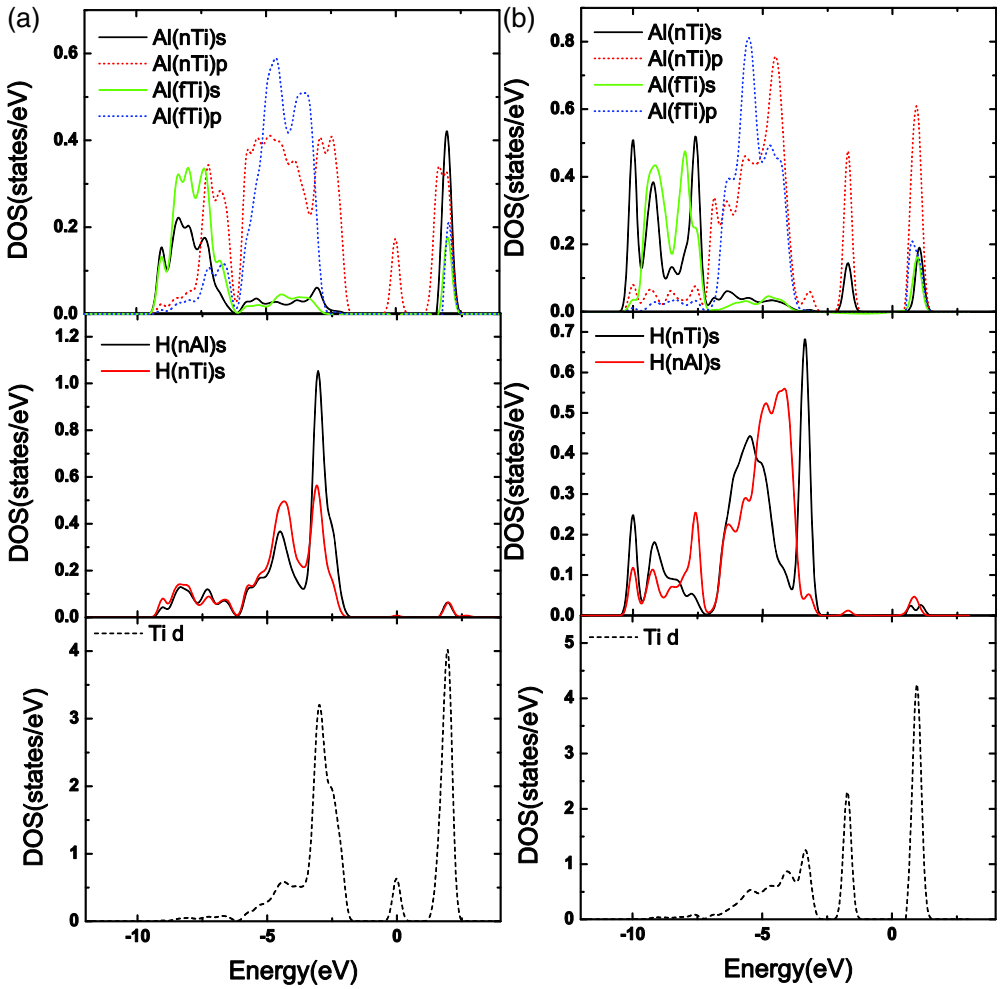

Figure 4. (Color online) Partial DOS of Na, Al, Ti and H atoms in (a) $Na_{16}Al_{15}TiH_{64}$ and (b) $Na_{16}Al_{15}TiH_{63}$. Solid, dotted and dashed lines denote s, p and d states, respectively. 'fTi' stands for 'far from the Ti dopant', which signifies a distance above 6.00 Å between Al and Ti atoms. 'nTi' and 'nAl' stand for 'near the Ti dopant' and 'near the Al atom', respectively. These signify distances shorter than 1.86 Å. The Fermi energy was set to zero.

that Na is still in the ionic form after doping. Considerable change is not observed in the DOS of H atoms far from the H vacancy.

Figures 4(a) and (b) show the DOS of the Ti-doped supercell after cluster substitution without and with a H vacancy in sodium alanate. The valence band of Al atoms far from the Ti atom exhibited little change upon substitution. Since Ti is at the left end of the transition series, its 3d states are much more like s and p valence states than those of other transition metals. Therefore, the 3d orbitals of Ti contribute to bonding with the surrounding atoms, resulting in a change in the valence band of Al and H atoms near the Ti atom, which is shown in figure 4(a). Moreover, the introduction of Ti dopant resulted in the formation of a metallic bond between Ti, Al and H atoms near the Ti atom. After the introduction of a H vacancy, all partial DOS, irrespective of whether they were near or far from the Ti dopant, shifted to lower energy, which caused the metallic bonds to disappear. It is this shift that causes the decrease in the enthalpies of formation and substitution of the $Na_{16}Al_{16}TiH_{63}$ supercell. The non-coincidence of the peaks of Ti, Al and H atoms indicates weakening of the bond strength, which occurs in the same manner as the changes in bond length discussed above.

4. Conclusions

Using first-principles calculations, we investigated the effects of doping Ti into sodium alanate, $NaAlH_4$, a hydrogen storage material. Lower formation enthalpy was found in the case of cluster substitution, in comparison with atom substitution. We demonstrated that substitution of a Ti atom for an Al atom in $Na_{16}Al_{15}TiH_{63}$ with inclusion of a H vacancy increased the stability of the structure. The Ti dopant made removal of the H atom from $NaAlH_4$ more energetically favorable. This result possibly explains the more facile desorption of hydrogen gas from Ti-doped sodium alanate. For the calculations on Ti-doped $Na_{16}Al_{16}H_{64}$, it was preferable to perform the initial substitution with a cluster of $TiAlH_n$. The appearance of $TiAl_3H_n$ in the supercell indicated that in bulk sodium alanate, the dehydrogenation of $Na_{16}Al_{16}H_{64}$ might start from a $TiAl_3H_n$ complex structure, and then decompose into $TiAl_3$. DOS analysis showed that the Ti atom bonds with the

surrounding atoms, thereby changing the valence band of the Al and H atoms near the Ti atom.

Acknowledgments

This work was supported by the New Energy and Industrial Technology Development Organization (NEDO) as an 'Advanced Fundamental Research Project on Hydrogen Storage Materials'. Some of the calculations were run on the AIST supercluster.

References

[1] Schlapbach L and Züttel A 2001 *Nature* **414** 353–8
[2] Pinkerton F E and Wicke B G 2004 *Indust. Phys.* **1** 20–3
[3] Yang J, Sudik A, Wolverton C and Siegel D J 2010 *Chem. Soc. Rev.* **39** 656
[4] Bogdanovic B and Schwickardi M 1997 *J. Alloys Compounds* **253** 1
[5] Majzoub E H and Gross K J 2003 *J. Alloys Compounds* **356/357** 363
[6] Sun D, Kiyobayashi T, Takeshita H T, Kuriyama N and Jensen C M 2002 *J. Alloys Compounds* **337** L8–11
[7] Bellosta von Colbe J M, Bogdanovic B, Felderhoff M, Pommerin A and Schüth F 2004 *J. Alloys Compounds* **370** 104
[8] Brinks H W, Jensen C M, Srinivasan S S, Hauback B C, Blanchard D and Murphy K 2004 *J. Alloys Compounds* **376** 215
[9] Íñiguez J, Yildirim T, Udovic T J, Sulic M and Jensen C M 2004 *Phys. Rev.* B **70** 060101
[10] Løvvik O M and Opalka S M 2005 *Phys. Rev.* B **71** 054103
[11] Aguayo A and Singh D J 2004 *Phys. Rev.* B **69** 155103
[12] Íñiguez J and Yildirim T 2005 *Appl. Phys. Lett.* **86** 103109
[13] Løvvik O M and Opalka S M 2006 *Appl. Phys. Lett.* **88** 161917
[14] Araújo C M, Ahuja R, Guillen J M O and Jena P 2005 *Appl. Phys. Lett.* **86** 251913
[15] Oriele P, Rosario C, Annalisa P, Jensen C M and Srinivasan S S 2005 *J. Phys. Chem.* B **109** 1168–73
[16] Íñiguez J and Yildirim T 2007 *J. Phys.: Condens. Matter* **19** 176007
[17] Ishibashi S, Terakura K and Hosono H 2008 *J. Phys. Soc. Japan* **77** 053709
[18] Perdew J P and Wang Y 1992 *Phys. Rev.* B **45** 13244–9
[19] Perdew J P, Burke K and Ernzerhof M 1996 *Phys. Rev. Lett.* **77** 3865–8
[20] Araújo C M, Li S, Ahuja R and Jena P 2005 *Phys. Rev.* B **72** 165101
[21] Hauback B C, Brinks H W, Jensen C M, Murphy K and Maeland A J 2003 *J. Alloys Compounds* **358** 142–5
[22] Bel'skii V K, Bulychev B M and Golubeva A V 1983 *Russ. J. Inorg. Chem.* **28** 1528
[23] Lauher J W, Dougherty D and Herley P J 1979 *Acta Crystallogr.* B **35** 1454–6
[24] Opalka S M and Anton D L 2003 *J. Alloys Compounds* **356/357** 486–9
[25] Wilson-Short G B, Janotti A, Peles A and Van de Walle C G 2009 *J. Alloys Compounds* **484** 347–51
[26] Felderhoff M, Klementiev K, Grünert W, Spliethoff B, Tesche B, Bellosta von Colbe J M, Bogdanovic B, Härtel M, Pommerin A, Schüth F and Weidenthaler C 2004 *Phys. Chem. Chem. Phys.* **6** 4369
[27] Graetz J, Reilly J J, Johnson J, Ignatov A Y and Tyson T Y 2004 *Appl. Phys. Lett.* **85** 500
[28] Liu J and Ge Q 2006 *Chem. Commun.* 1822–4
[29] Liu J and Ge Q 2006 *J. Phys. Chem.* B **110** 25863
[30] Schuth F, Bogdanovic B and Felderhoff M 2004 *Chem. Commun.* 2249–58
[31] Blomqvist A, Araújo C M, Jena P and Ahuja R 2007 *Appl. Phys. Lett.* **90** 141904
[32] Rao B K, Jena P, Burkart S, Ganteför G and Seifert G 2001 *Phys. Rev. Lett.* **86** 692
[33] Kumar K S 1990 *Powder Diffract.* **5** 165